Time-Resolved Spectroscopic Measurements of High Density in Ar-Filled Microballoon Implosions

C. F. Hooper, Jr., D. P. Kilcrease, R. C. Mancini, and L. A. Woltz[a]
Department of Physics, University of Florida, Gainesville, Florida 32611

D. K. Bradley, P. A. Jaanimagi, and M. C. Richardson
Laboratory for Laser Energetics, University of Rochester, Rochester, New York 14623
(Received 21 November 1988)

We report on the analysis of time-resolved x-ray spectra from direct-drive, Ar-filled polymer-shell implosion experiments in which we trace the time evolution of the electron density through stagnation. Very high electron densities in the range $(2-8)\times10^{24}$ cm^{-3} are inferred. We also discuss several novel spectral features, including large Stark broadening of satellite line emission, optical thicknesses for resonant transitions lower than expected, and the onset of density-dependent "blue satellites" on the high-energy wing of the He_α line.

PACS numbers: 52.25.Nr, 32.70.−n, 52.50.Jm, 52.70.La

In current high-density laser-driven implosion experiments the determination of core conditions at implosion is of great importance. This is particularly true for experiments concerned with fusion (D_2- or DT-filled targets) where nuclear diagnostics have been developed to estimate final core conditions.[1,2] A complementary approach relying on x-ray spectroscopy of high-Z gases (as total fill gas or as dopant) provides values of electron density and temperature.[3] This technique has the added advantage that with the inclusion of x-ray streak-camera technology, these parameters can be followed in time during the implosion. These experiments also provide an opportunity to generate and study spectroscopically the basic properties of highly charged ions in dense plasmas. Today, the need to model the spectra produced by highly charged ions has motivated a resurgence of interest in certain areas of atomic physics; particularly interesting, as the density increases, is the interplay between atomic and plasma physics where independent atomic and plasma descriptions are no longer adequate. For example, we were able to compute accurate Stark-broadened red satellite line profiles by including the details of the interaction between doubly excited states and the plasma. This newly developed capability has proved to be crucial in the spectroscopic determination of the high densities achieved in these experiments. Further, we conjecture that the appearance of density-dependent blue satellite features, as yet unexplained, is the signature of collective radiator behavior. Finally, the observation of moderately optically thick K-shell lines under very-high-density conditions is significant in itself.

In this paper, we report the time-resolved spectroscopic analysis of compressed high-Z-gas-filled targets. In a series of experiments performed at the University of Rochester's Laboratory for Laser Energetics, Ar-filled plastic microballoons of dimensions $420\,\mu\text{m}\times6\,\mu\text{m}$ (diameter×wall thickness) were imploded using the 24-beam uv ($\lambda=0.35\,\mu$m) Omega laser system, operated with maximum illumination uniformity afforded by new distributed-phase-plate technology.[4] Total incident laser energy was 1700 J and its Gaussian pulse duration (FWHM) was 680 ± 50 ps. The targets were filled to pressures of 2 and 10 atm of Ar. A broad array of diagnostics included time-resolved x-ray line spectroscopy with SPEAX curved-crystal streak spectrograph[5] and time-integrated x-ray imaging of the compressed core. In Figs. 1 and 2, we show spectra recorded on two shots at different target pressures. The energy range displayed

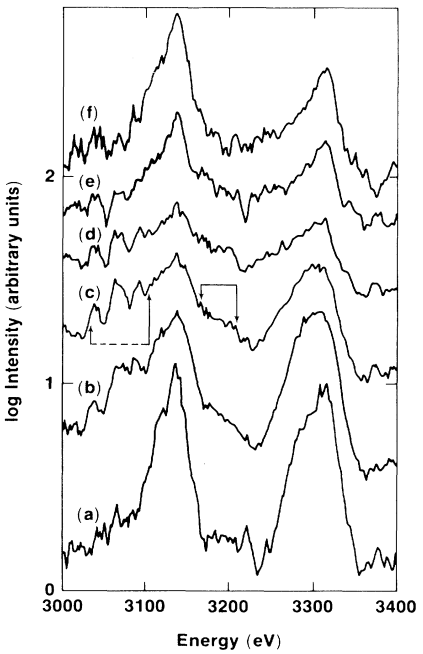

FIG. 1. Series of time-resolved spectra for the 2-atm case. (c) and (d) correspond to implosion stagnation. (---) inner-shell transitions in C-, B-, and Be-like Ar; (⟶) broad "blue satellite" feature. These spectra have been shifted vertically by arbitrary amounts for the purpose of suitable display in the same picture.

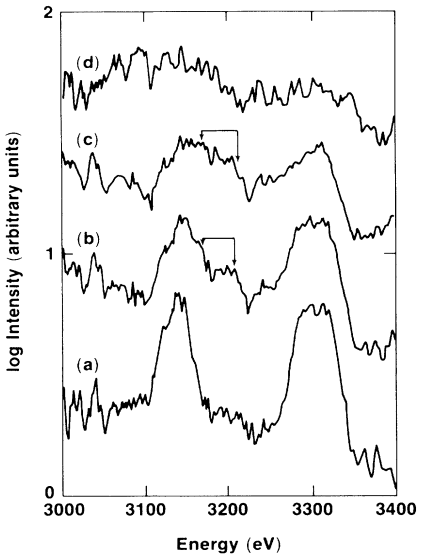

FIG. 2. Same as in Fig. 1, but for the 10-atm case. In this case, spectrum (c) is characteristic of the stagnation. Note that after the stagnation, (d), only continuum emission is seen.

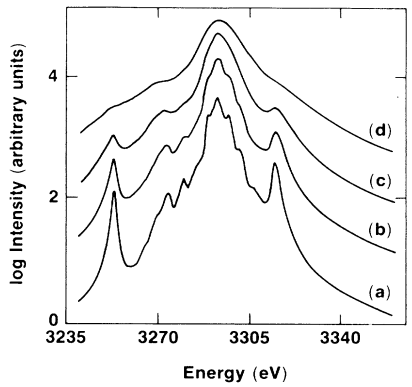

FIG. 3. He-like satellite line profiles for Ar^{+16} for an electron temperature $T_e = 800$ eV and densities of (a) $N_e = 5\times10^{23}$ (b) 1×10^{24}, (c) 2×10^{24}, and (d) 5×10^{24} in cm^{-3}.

covers emission from the He_α and L_α transitions of He- and H-like Ar and their associated satellite structure. Emission from the He_β and L_β lines was too weak for spectroscopic analysis; higher members of the helium and Lyman series either were not seen or lie beyond the energy range covered by the spectrograph. Spectra recorded from the implosion of an empty target determined the extent of instrument-generated structure in the continuum background. Both Figs. 1 and 2 show a time sequence of spectra integrated over 60-ps intervals at different times through the final stages of the implosion. The He-like satellites ($2l2l'$-$1s2l$) of L_α are very intense and together with the L_α line give rise to the spectral feature located around 3300 eV, whose low-energy side is dominated by satellite transitions and high-energy side by the L_α line. Since the line shapes of the satellite and resonant transitions have been broadened sufficiently to cause merging, it is not possible to resolve the separate features as was possible in previous implosion experiments.[6-9] As the implosion progresses, the overall shape of this composite spectral feature broadens further and also shows varying degrees of asymmetry. The spectral feature associated with the He_α line and its Li-like satellites also shows an interesting evolution; as the time advances we see the onset of an unusual emission feature or band (~3160–3220 eV) on the blue or high-energy wing of the He_α line in addition to the usual red satellites ($1s2l2l'$-$1s^2sl$) found on the low-energy wing. This blue feature appears in both Figs. 1 and 2, although more prominently in the second one where it achieves its highest intensity at the time of stagnation when the maximum density is reached. For the target with the lower fill pressure, the feature is weaker but most evident at stagnation. In Fig. 1 we notice, between 3040 and 3100 eV, three emission peaks corresponding to inner-shell transitions in C-, B-, and Be-like argon. The evolution of their intensity can be observed before and at the implosion's stagnation. In Fig. 2 we see the red wing of the He_α line partially truncated as the implosion approaches stagnation. We interpret this as in incipient absorption feature due to transitions in lower ionization stages.

These spectra are compared to Stark- and opacity-broadened theoretical line profiles to provide a history of the electron density and temperature during the implosion. The Stark-broadened line profiles were computed for the L_α line of H-like Ar and its He-like satellite transitions using a recently developed multielectron line profile code.[10] In previous spectroscopic diagnostics based on satellite analysis, the satellite line profiles were approximated by Voigt profiles. However, we find that as the density increases, Stark-broadening and field-mixing effects become more important and can introduce substantial changes to the usually assumed Voigt satellite line shapes. For example, in Fig. 3 we show a series of Stark-broadened satellite line profiles computed for increasing values of the electron density. The calculation involves all the transitions between He-like double-excited $2l2l'$ states, the relative population distribution of which was taken to be in local thermodynamic equilibrium (LTE), and single-excited $1s2l$ states. The Stark broadening is treated by the Smith-Hooper relaxation theory with the static ion approximation.[10] The fitting of the spectral feature associated with the L_α line and its related satellite emission is done by using an intensity model that combines the calculated line profiles of satellite and resonance transitions. Opacity broadening is simulated in each line profile by means of the uniform-slab model and is characterized by the optical thickness at line center τ_{0s} (satellite) and τ_{0r} (resonance).[6] Doppler and instrumental broadening are also included.

Before the experimental spectra are compared with the theoretical calculations, the continuum background, estimated from the spectrum over a broader energy range, is subtracted. For a given spectrum and value of the electron density N_e, we pick τ_{0r} and τ_{0s} for the best possible fit of the experimental data subject to the constraint indicated below; this is done by minimizing the sum of the square differences between experimental and theoretical log-intensity points (Q^2). This procedure is repeated for different values of N_e allowing us to see the changes in Q^2 and the values of τ_{0r} and τ_{0s} as a function of N_e. We find for each spectrum that there is a range of N_e over which Q^2 has a minimum, and where the quality of the fit is very good. Next, the ratio of optical thicknesses τ_{0r}/τ_{0s} obtained from Q^2 minimization can be checked for consistency with the values computed using kinetic modeling for the same N_e. This ratio minimizes any uncertainty in the assumption of a characteristic geometrical length and is proportional to the ratio of populations in the lower state of each transition. Independently, a collisional-radiative kinetic code was also used to compute this ratio.[11] We have therefore examined the sensitivity of this ratio to different modeling assumptions such as optically thin, optically thick, LTE, or changes in the number of excited states. For electron densities greater than 1×10^{24} cm^{-3} this ratio is rather insensitive to modeling details and becomes a function only of N_e and T_e. This is because at these high densities, the $n=2$ level of He-like Ar gradually comes into equilibrium (LTE) with the ground state ($n=1$) of H-like Ar although, for example, this ground state is *not* in LTE with the $n=2$ level of H-like Ar. Comparison with kinetic calculations also lets us estimate values of the electron temperature T_e. A similar study of the spectral feature associated with the He$_\alpha$ line and its Li-like satellite transitions was performed in order to check consistency with the results of the L$_\alpha$ spectral feature. An analysis of the data in Figs. 1 and 2 based on the above procedure allows us to infer N_e and T_e. Table I summarizes our findings. As an example, Fig. 4 shows the experimental data, the continuum background level, and several theoretical fits. The result at $N_e=5\times10^{24}$ cm^{-3} is representative of the best simultaneous fit to the He$_\alpha$ and L$_\alpha$ spectral features. The energy intervals used in the fits are 3100–3170 eV (He$_\alpha$) and 3260–3340 eV (L$_\alpha$). The smooth transition in between is due to extrapolation of both wings. At $N_e=1\times10^{24}$ and 8×10^{24} cm^{-3}, the fits to the L$_\alpha$ spectral feature deteriorate and the Q^2 values are over 10 times the Q^2 for 5×10^{24} cm^{-3}; at $N_e=2\times10^{24}$ cm^{-3} (not shown in Fig. 4) the fit is still not as good as at 5×10^{24} cm^{-3} and Q^2 is 7 times larger. For the He$_\alpha$ spectral feature the worst fits occur at the lower densities.

It is important to note that the values of τ_{0r} (5–20) for the L$_\alpha$ line deduced in the fitting procedure are significantly smaller than those required to fit the spectra from previous experiments.[6] One-dimensional hydrodynamic simulations of these experiments indicate that close to stagnation a central region of about 25% of the Ar mass is sufficiently hot to populate the K-shell ions; the remaining Ar has a temperature in the range 200–600 eV.[11,12] While the gradients across the entire mass of Ar may be larger we find that within the small central region they are significantly less severe. Hence, to describe the opacity broadening in this region we employed the uniform-slab model. We estimate that effects of temperature and density gradients could introduce uncertainties on the order of 50% in our density inferences.[13] Ionization-balance calculations performed in the temperature range 200–600 eV characteristic of the outer region for densities >4 g cm^{-3} indicate C-, B-, Be-, and Li-like ions share almost all the population ($<80\%$).[14] Also, the population of excited states becomes comparable to or even exceeds that for the ground states as the density increases. Hence, we estimate the

TABLE I. Density and temperature results for the analysis of data in Figs. 1 and 2. Time is measured with respect to the peak of the laser pulse (1×10^{24} cm$^{-3}\simeq4$ g cm^{-3}).

Spectrum	Time interval (ps)	Electron density (10^{24} cm^{-3})	Temperature (eV)
Fig. 1(a)	109–171	2–6	600–900
(b)	171–233	4–6	600–900
(c)	202–264	4–7	600–800
(d)	233–295	6–8	500–600
(e)	295–357	2.5–6	450–600
(f)	357–419	2.5–4	450–600
Fig. 2(a)	312–375	3–6	600–900
(b)	348–405	5–7	600–800
(c)	375–427	6–8	500–800

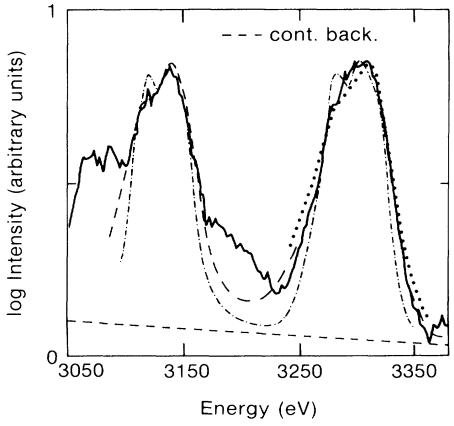

FIG. 4. An example of the fittings obtained. This case corresponds to spectrum (b) in Fig. 1. Experimental spectrum (——); theoretical fittings: $N_e=1\times10^{24}$ (-·-·), 5×10^{24} (---), and 8×10^{24} (····), in cm^{-3}.

optical thicknesses of the L_α spectral feature in the central hot core at $T_e = 800$ eV and $N_e = 5 \times 10^{24}$ cm^{-3} to be in the ranges $\tau_{0r} = 18$–30 and $\tau_{0s} = 6$–10 with a ratio $\tau_{0r}/\tau_{0s} = 3$; on the other hand, from our analysis of best fit we obtain $\tau_{0r} = 16$ and $\tau_{0s} = 5$.

Estimates based on the time-integrated pinhole x-ray (2–4 keV) images of the compressed core are also in reasonable agreement with our spectroscopic analysis, showing a spherically symmetric imploded Ar plasma of diameter 35 μm. Assuming Ar mass conservation, this would indicate average mass densities of 20–40 g cm^{-3}.

In conclusion, the electron densities recorded here are the largest observed directly through spectroscopic means. Furthermore, resonance lines with lower than expected optical thicknesses are consistent with our modeling and imply that under these conditions K-shell lines can still be observed and analyzed in very dense plasmas. Since the spatial extent of the excited-state orbitals at these densities is comparable to the average interatomic spacing, the onset of the blue satellite features may indicate the initiation of a plasma-solid phase transition.[15] However, additional analysis is required to verify this speculation.

---

[a]Presently at the National Bureau of Standards, Gaithersburg, MD 20899.

[1]S. Skupsky and S. Kacenjar, J. Appl. Phys. **52**, 2608 (1981).

[2]E. G. Gamalii, S. Yu. Gus'Kov, O. N. Krokhim, and V. B. Rozenov, Pis'ma Zh. Eksp. Teor. Fiz. **21**, 156 (1975) [JETP Lett. **21**, 70 (1975)].

[3]B. Yaakobi, S. Skupsky, R. L. McCrory, C. F. Hooper, Jr., H. Deckman, P. Bourke, and J. M. Soures, Phys. Rev. Lett. **44**, 1072 (1980).

[4]Laboratory for Laser Energetics Quarterly Review **33**, 1 (1987).

[5]B. L. Henke and P. A. Jaanimagi, Rev. Sci. Instrum. **56**, 1537 (1985).

[6]N. D. Delamater, C. F. Hooper, Jr., R. J. Joyce, L. A. Woltz, N. M. Ceglio, R. L. Kauffman, R. W. Lee, and M. C. Richardson, Phys. Rev. A **31**, 2460 (1985).

[7]A. Hauer, K. B. Mitchell, D. B. van Hulsteyn, T. H. Tan, E. J. Linnebur, M. M. Mueller, P. C. Kepple, and H. R. Grien, Phys. Rev. Lett. **45**, 1495 (1980).

[8]M. H. Key, C. L. S. Lewis, J. G. Lunney, A. Moore, J. M. Ward, and R. K. Thareja, Phys. Rev. Lett. **44**, 1669 (1980).

[9]C. F. Hooper, Jr., R. C. Mancini, D. P. Kilcrease, L. A. Woltz, M. C. Richardson, D. K. Bradley, and P. A. Jaanimagi, Proc. SPIE Int. Soc. Opt. Eng. **913**, 129 (1988).

[10]L. A. Woltz and C. F. Hooper, Jr., Phys. Rev. A **38**, 4766 (1988).

[11]R. C. Mancini and C. F. Hooper, Jr., J. Phys. D **21**, 1099 (1988).

[12]J. Delettrez (private communication).

[13]R. W. Lee, J. Quant. Spectrosc. Radiat. Transfer **27**, 87 (1982).

[14]Y. T. Lee, J. Quant. Spectrosc. Radiat. Transfer **38**, 131 (1987).

[15]S. M. Younger, A. K. Harrison, K. Fujima, and D. Griswold, Phys. Rev. Lett. **61**, 962 (1988).